Evaluating Mathematical Models for Mixed-Substrate Bacterial Growth in a Chemostat

Aishani Sinha, Freya Bull

July 2024

Abstract

Models currently exist that effectively capture the dynamics of nutrient-limited, single-substrate bacterial growth in a well-mixed, constantly diluted volume, known as a chemostat. These models, that describe bacterial growth on a single substrate, are of great practical importance in numerous industries, ranging from pharmaceutical production and food/drink manufacturing to waste water treatment. However, in nature it is rare for nutrients to be present in the environment as a singular substrate; more often than not, bacteria will grow on a mixture of many different substrates. Given this, there is a need for a mathematical model that effectively describes the dynamics of mixed-substrate bacterial growth. In this paper, we use data from experiments conducted in 1996 by Lendenmann, Snozzi and Egli on the growth of *Escherichia coli* on different sugar mixtures to evaluate the suitability of various mathematical models. To do so, a computational framework, written in Python, was developed to quantify the differences between the experimentally obtained values and theoretically calculated values for different variables in the chemostat setup. Each bacterial growth model explored in this research builds upon the previous through the addition of higher-order interactive relationships between the individual substrates. We begin with a rudimentary model that assumes that the bacteria consume the individual substrates sequentially, and later progress to a more complex model that incorporates interaction parameters to consider the inhibitory effect that each substrate has on the others. The results from this analysis suggest that the higher-order growth rate models, which account for an interaction effect between substrates, are more suitable for describing multi-substrate growth; highlighting the complexity of the mechanisms underlying bacterial growth.

1 Introduction

A chemostat is a well-mixed, continuously diluted volume contained within a vessel, in which growth substrate is externally supplied from a reservoir at a constant flow rate, and from which a mixture of bacteria and spent substrate is removed at the same rate, maintaining a constant volume within. The steady-state population in the chemostat is reached when the rate of bacterial growth is equivalent to the dilution rate, creating an environment in which bacteria grow at exactly the rate at which they are removed [1].

Chemostats are widely used in a number of industries, including wastewater treatment and pharmaceutical production. Recent FDA approvals for drugs produced by continuous cultivation will likely see an increase in the utilisation of continuous bioprocesses by the pharmaceutical industry, via biological devices like the chemostat. It is likely that other industries, such as the food and drink manufacturing industry, will follow suit given that continuous production offers far greater volumetric productivity, and as a consequence, reduced expenditure in equipment [2].

1.1 Monod Growth Model

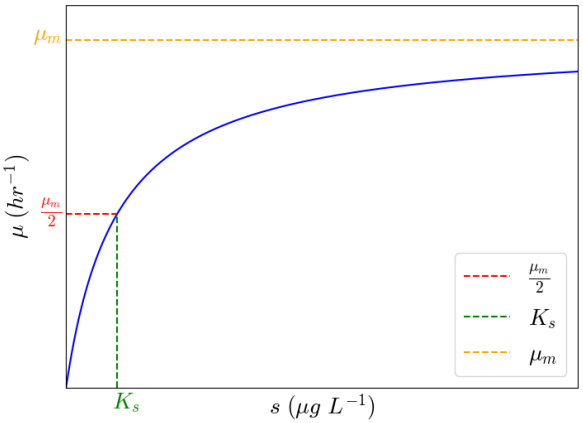

Figure 1: Illustration of the Monod Growth model (equation 1). In blue is the growth rate, μ, as a function of the single substrate concentration, s. At the substrate concentration K_s (green), the growth rate is half (red) of its maximum value, μ_m (yellow).

Bacterial growth in a chemostat is commonly modelled as a function of substrate concentration, described by the empirical Monod relation as fol-

lows [3]:

$$\mu(s) = \frac{\mu_m s}{s + K_s} \tag{1}$$

In this equation, μ describes the specific bacterial growth rate, s is the concentration of the single substrate, μ_m is the maximum bacterial growth rate, and K_s is the saturation constant, which is the substrate concentration at which the bacterial growth rate is half of the maximum growth rate. Importantly, K_s and μ_m are properties that are specific to a particular substrate. Equation 1 is represented graphically in figure 1, illustrating how the bacterial growth rate varies with the substrate concentration.

1.2 Single substrate chemostat dynamics

In the case of bacterial growth on a single substrate, ordinary differential equations can be written to define a relationship between the growth of a bacterial population to the concentration of a single limiting nutrient (the substrate) [4].

Considering mass balance equations for the bacterial mass and substrate mass in the chemostat leads to the following equations for the bacterial concentration and substrate concentration:

$$\begin{aligned} \frac{d\rho}{dt} &= (\mu - D)\,\rho \\ \frac{ds}{dt} &= D\,(s_0 - s) - \frac{\mu\rho}{Y} \end{aligned} \tag{2}$$

Here, ρ is the bacterial concentration, μ is the bacterial growth rate (as specified by equation 1), D is the dilution rate, s is the substrate concentration, s_0 is the externally inputted substrate concentration, and Y is the bacterial yield, set by $dp = Y ds$.

The steady state solution is obtained when the rate of change in concentration is zero (i.e. $\frac{d\rho}{dt} = 0$, $\frac{ds}{dt} = 0$):

$$\begin{aligned} \tilde{\mu} &= D \\ \tilde{s} &= \frac{K_s D}{\mu_m - D} \\ \tilde{\rho} &= Y\left(s_0 - \frac{K_s D}{\mu_m - D}\right) \end{aligned} \tag{3}$$

A key limitation of the ordinary differential equations presented above is that they consider bacterial growth on a single substrate, assuming a Monodic growth rate. The aim of this report is to evaluate various models that extend this model to consider the dynamics of mixed-substrate growth.

1.3 The Dataset

The evaluations of mathematical models discussed in this report are made possible through results obtained by experiments conducted by Lendenmann, Snozzi and Egli on the growth of *Escherichia coli* on various sugar mixtures in chemostats in their 1996 paper [5]. This dataset details bacterial growth on different combinations of the following substrates, where in brackets is the abbreviation for each: glucose (glc), galactose (gal), maltose (mal), ribose (rib), arabinose (ara) and fructose (fru).

The results from each of these experiments are collated in Lendenmann and Egli's 1998 paper [6], and can be found in the appendix (figure 4), with additional supplementary information (figure 5) detailing the values of μ_m and K_s for each substrate.

2 Sequential Uptake Model

The simplest multi-substrate model assumes the sequential (one by one) uptake of individual substrates, with bacteria simply switching substrates when they have depleted one substrate enough that another becomes more favourable. This results in a mechanism whereby individual substrates are depleted in growth rate order, depending on which one provides the highest instantaneous growth rate.

Mathematically, this sequential uptake for growth on n substrates can be written as:

$$\mu(t) = \max\{\mu_1(t), \mu_2(t), ..., \mu_n(t)\} \tag{4}$$

where $\mu_i(t)$ is a function of time for the growth rate of the i^{th} substrate in the mixture.

This growth rule implies that the bacterial concentration steady state attained by growth on each individual substrate independently is additive, and the sum of these steady states should be equivalent to the overall bacterial steady state (given by the Dry Weight column in the dataset). This can be mathematically expressed as below:

$$\tilde{\rho} = \sum_{i=1}^{n} \tilde{\rho}_i \tag{5}$$

where $\tilde{\rho}_i$ is the theoretical bacterial steady state from growth on the i^{th} substrate independently, and $\tilde{\rho}$ is the overall bacterial steady state in the chemostat.

Substituting the equation for the steady steady solution of bacterial concentration (equation 2), this can be written further as:

$$\tilde{\rho} = \sum_{i=1}^{n} Y_i(s_{0;i} - \tilde{s_i}) \tag{6}$$

where for each substrate i: Y_i is the yield coefficient, $s_{0;i}$ is the input concentration, and $\tilde{s_i}$ is the steady state concentration.

From the dataset previously discussed, all variables required for equation 6 are experimentally determined, except for the substrate yield coefficients.

Thus, we use the experimental data to calculate the yield coefficient for each of the n substrates in each experiment using optimisation methods. We then compare the obtained values across the different experiments, to determine if the yield coefficients calculated for each substrate are similar across the experiments.

To illustrate this methodology, we here present our approach for Rows 1-6 in the dataset, concerning the growth of *E. coli* on mixtures of glucose and galactose sugars at varying ratios. In this case, equation 6 can be written as below:

$$\tilde{\rho} = Y_{glc}(s_{0;glc} - \tilde{s}_{glc}) + Y_{gal}(s_{0;gal} - \tilde{s}_{gal}) \quad (7)$$

where *glc* and *gal* represent the sugars glucose and galactose respectively. We now can substitute the values for $\tilde{\rho}$, $s_{0;glc}$, $\tilde{s}_{glc}$, $s_{0;gal}$, and $\tilde{s}_{gal}$ from the dataset (figure 4), and obtain values for Y_{glc} and Y_{gal} through curve fitting with non-linear least squares.

	1-12	**13-18**	**19-24**	**25-30**
Glc	0.4616	0.4790	0.4863	0.4906
Gal	0.5151	0.4422	-	-
Mal	-	0.5449	-	-
Rib	-	0.4680	-	-
Ara	-	0.4817	0.4551	-
Fru	0.3558	0.4684	-	0.4543

Table 1: The values of the yields, Y obtained by fitting equation 6. Each column represents a different experiment, here referred to by the corresponding rows in the dataset, while each row is a sugar (substrate) for which the yield is calculated.

Table 1 shows the results of fitting the yield parameters for each experiment in the dataset. All values obtained for the yield coefficients are between 0 and 1 which indicates that the substrate utilisation rate is greater than bacterial growth rate, as one would expect.

Note that solving for the yields of glucose, galactose and fructose in rows 7-12 would be an issue, as the steady state values for glucose remain fixed while glucose and galactose change, and so solving for 3 yield values would result in an undetermined system. As a result, we amalgamated rows 1-6 and rows 7-12 to avoid this and ensure that all 3 variables can be solved for with the data.

Whilst the yield values seem reasonable when considering each experiment in isolation ($0 \leq Y_i \leq 1$), it is clear that the yields obtained per substrate are variable and not constant, as the sequential uptake model would expect. Hence, there is a need to investigate a different model, which leads us to the the next section.

3 Lendenmann Ratio Model

In 1996, based on experimental results, Lendenmann proposed a model wherein the steady-state concentrations of individual sugars are proportional to their contributions to the total substrate concentration in the input growth medium [5]. This model assumes that the bacterial growth on each substrate remains that of a single substrate model, for example the Monod relation. Considering an arbitrary substrate, s_1, this ratio relation can be written as:

$$\tilde{s_1} = s_{1;100\%} \cdot \frac{s_{0;1}}{\sum_{i=1}^{n} s_{0;i}} \quad (8)$$

Here, $\tilde{s_1}$ is the steady state concentration of s_1, $s_{1;100\%}$ is the theoretical steady state substrate concentration from the single growth model and $s_{0;i}$ is the input concentration of the i^{th} substrate. In the following subsections, we will consider two different single-substrate bacterial growth equations, the Monod equation and the Moser equation, and then evaluate the Lendenmann Model using each model.

3.1 Monod Growth Model

In Section 1.1, we presented the Monod growth model for bacterial growth on a single substrate. By using the expression for $\tilde{s}$ from the Monod model (equation 3), we can rewrite the Lendenmann model (equation 8) as:

$$\tilde{s_1} = \frac{K_s D}{\mu_m - D} \cdot \frac{s_{0;1}}{\sum_{i=1}^{n} s_{0;i}} \quad (9)$$

The dataset provides values for the steady state concentration of each substrate in different proportions in the mixtures, allowing the predictions of equation 9 to be directly compared to the experimentally determined values.

There is a degree of uncertainty in both the experimental and theoretical values for this model. For the experimental steady state substrate concentration, we use an uncertainty of 10%, derived from the variance in experimental data, as stated in Lendenmann's 1994 thesis [7]. The uncertainty in the predicted values of $\tilde{s}$ can be calculated from the errors in K_s, D, and μ_m, as below.

$$\frac{\Delta\tilde{s}}{\tilde{s}} = \sqrt{\left(\frac{\Delta K_s}{K_s}\right)^2 + \left(\frac{\Delta \mu_m}{\mu_m}\right)^2 + \left(\frac{\Delta D}{D}\right)^2} \quad (10)$$

Again, the uncertainties in K_s are given in the 1994 paper, and because the values for K_s and μ_m were obtained in conjunction with one another, the uncertainty in μ_m is implicit in that of K_s. The error in D is further derived from the variance of results, and is 5%, leading to the general formula for the uncertainty:

$$\frac{\Delta\tilde{s}}{\tilde{s}} = \sqrt{\left(\frac{\Delta K_s}{K_s}\right)^2 + (0.05)^2} \quad (11)$$

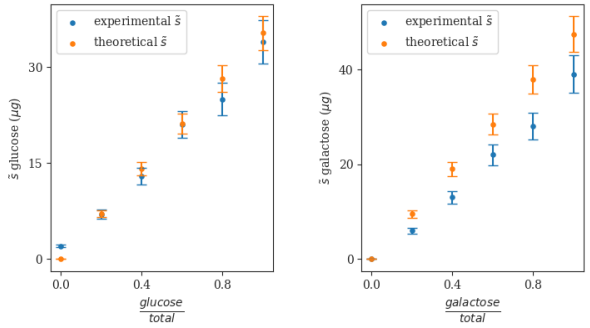

(a) Steady states 1-6 from dataset

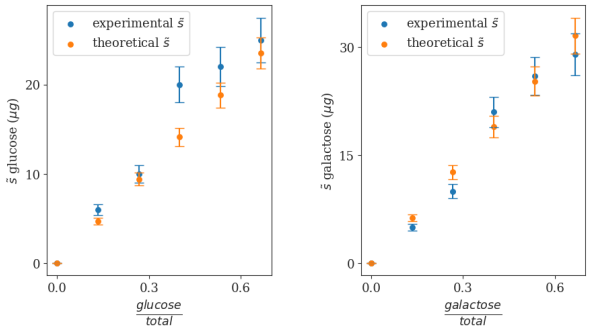

(b) Steady states 7-12 from dataset

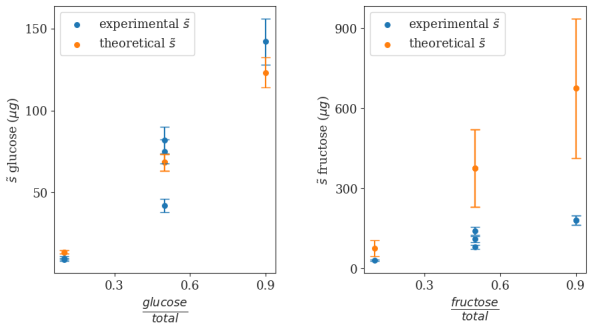

(c) Steady states 25-30 from dataset

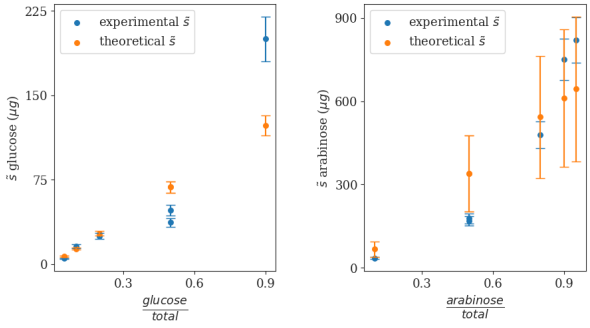

(d) Steady states 19-24 from dataset

Figure 2: Comparing the experimentally observed steady state substrate concentration (blue) for individual substrates in different mixtures to the theoretical steady states (orange) predicted by the Lendenmann model (equation 9).

Figure 2 plots the predicted values of the steady states against the experimentally determined steady states. As expected, there is a linear relationship between the substrate proportions and theoretical steady state substrate concentrations, and it is promising to see a similar linear relationship exhibited between the substrate proportions and the experimental values. In order to evaluate whether a strictly linear relationship is present between the substrate ratios and experimental steady state concentrations, we calculated the Pearson Correlation Coefficient (PCC) for each substrate in the different experiments, shown below:

Dataset	Substrate	PCC
1-6	glucose	0.9959
	galactose	0.9959
7-12	glucose	0.9813
	galactose	0.9873
19-24	glucose	0.9005
	fructose	0.9344
25-30	glucose	0.9588
	arabinose	0.9460

Table 2: The Pearson Correlation Coefficient for each substrate from each experiment in the dataset.

As can be seen in table 2, the values for the Pearson Coefficient Correlation are all > 0.90, which suggests a strongly linear relationship between the substrate ratio and the steady state substrate concentration. This strongly linear relationship, combined with the fact that the discrepancies in the theoretical and experimental values are largely accounted for by the uncertainty in both quantities suggests that the model fairly suitably captures the mixed-substrate growth, but one might expect a more complex relationship to be governing the interaction between substrates.

3.2 Moser Growth Model

The Monod growth equation is just one model for bacterial growth on a single substrate – other models have been proposed, such as the Moser model which also aims to capture this growth. In this section, we will use the Moser growth model to describe a single substrate within the Lendenmann model (equation 8), and thus investigate the effect of substituting the growth model on the validity of the Lendenmann Model.

Introduced by Herman Moser in 1958, this model extends the Monod model by introducing an exponential fitting parameter n, which modifies the Monod relation as follows [8]:

$$\mu = \frac{\mu_{max} s^n}{K_s + s^n} \tag{12}$$

As before, the steady state solution for the substrate

concentration can be found by setting $\mu = D$,

$$\tilde{s} = \left(\frac{DK_s}{\mu_{max} - D}\right)^{\frac{1}{n}} \tag{13}$$

and substituting this expression into the Lendenmann model (equation 8) gives the following:

$$\tilde{s_1} = \left(\frac{DK_s}{\mu_{max} - D}\right)^{\frac{1}{n}} \cdot \frac{s_{0;1}}{\sum_{i=1}^{n} s_{0;i}} \tag{14}$$

Equation 14 can be manipulated to produce a linear relationship, as seen in equation 15. This relationship can now be applied to calculate n via orthogonal distance regression on the dataset.

$$\ln\left(\frac{DK_s}{\mu_{max} - D}\right) = n\left(\ln \tilde{s_1} \frac{\sum_{i=1}^{n} s_{0;i}}{s_{0;1}}\right) \tag{15}$$

Substrate	**Dilution Rate** (hr^{-1})	n
Glucose	0.3	0.994 ± 0.002
	0.3	1.020 ± 0.006
	0.6	0.990 ± 0.020
	0.6	0.991 ± 0.013
Galactose	0.3	0.968 ± 0.002
	0.3	0.994 ± 0.009
Fructose	0.3	1.033 ± 0.008
	0.3	0.852 ± 0.009

Table 3: Values of the exponential fit parameter n obtained via optimisation methods for each substrate in the different experiments, with calculated uncertainties, obtained by considering the errors of the variables within the logarithmic terms.

Table 3 shows the resultant values of n obtained by regression. The values of n do not significantly deviate from $n = 1$ (the Monod model), which supports the idea that the adjustments to the Monodic growth rate through the fitting term do not alter the suitability of the Lendenmann model.

4 Interaction models

The previous models we explored do not directly account for the complex interactions between substrates during bacterial growth, and instead assume that bacterial growth on each individual substrate occurs independently. However, a more realistic assumption has some interaction occurring between the substrates: either competitive, inhibitory or mutualistic.

4.1 Generalised Interaction Model

In 1977, Yoon et al. proposed a model that accounted for pairwise interactions between individual substrates in dual-substrate bacterial growth [9]. The bacterial growth rate is modelled as a function of both individual substrate concentrations, s_1 and s_2, as follows:

$$\mu(s_1, s_2) = \frac{\mu_{m;1} s_1}{K_{s;1} + s_1 + a_{12} s_2} + \frac{\mu_{m;2} s_2}{K_{s;2} + s_2 + a_{21} s_1} \tag{16}$$

In this dual-substrate growth rate equation, which is derived from considering enzyme kinetics, each substrate exhibits a competitive inhibition effect on the utilisation of the other substrate, where the extent of this effect is quantified by interaction parameters a_{12} and a_{21}. Concretely, a_{12} represents the inhibition effect of the first substrate on the second and the converse for a_{21}. This degree of interaction in this model is defined by the proportion of saturation constants between both individual substrates, which can be seen below to:

$$\mu(s1, s2) = \frac{\mu_{m;1} s_1}{K_{s;1} + s_1 + \frac{K_{s;1}}{K_{s;2}} s_2} + \frac{\mu_{m;2} s_2}{K_{s;2} + s_2 + \frac{K_{s;2}}{K_{s;1}} s_1} \tag{17}$$

This equation can be generalised to account for *all* pairwise interactions across n substrates, as shown below:

$$\mu = \sum_{i=1}^{n} \frac{\mu_{m;i} s_i}{K_{s;i} + \sum_{i=1}^{n} a_{ij} s_j} \tag{18}$$

In this model, a_{ij} represents the inhibition effect of the j^{th} substrate on the uptake of the i^{th} substrate by the bacteria. If $a_{ij} = 1$, this means that the j^{th} substrate has the same saturation effect as the i^{th} substrate has on itself: a competitive interaction. If $a_{ij} > 1$, then the j^{th} substrate has an inhibitory effect on the uptake of the i^{th}. If $a_{ij} < 1$, the interaction is mutualistic.

By considering the generalised dual-substrate growth rate model of equation 16, the interaction parameters a_{12} and a_{21} can be fit to the experimental data. This is achieved by considering the steady state solution $\tilde{\mu} = D$, i.e. by equating $\mu(s_1, s_2) = D$ for each row in the dataset, and using non-linear least squares methods to estimate the interaction parameters. These obtained values can then be compared to the theoretical expression for a_{12} and a_{21}, to determine whether interactions are indeed determined by the proportion of saturation constants. These results are shown in table 4.

Dataset	a_{12}		a_{21}	
	Fit	$\frac{K_{s;1}}{K_{s;2}}$	**Fit**	$\frac{K_{s;1}}{K_{s;2}}$
1-6	-9.04	0.745	2.8507	1.34
19-24	0.257	0.553	0.6176	1.81
25-30	-0.277	0.585	0.319	1.71

Table 4: Comparison of the fitted interaction parameters with the theoretically predicted ratio of saturation constants. These interaction parameters were calculated for each dual-substrate experiment.

Table 4 indicates no similarity between the values of fitted interaction parameters and the theoretically expected values. This is likely due to the number of variables involved, combined with the lack of data, but it is also possible that the saturation effect on one another is not the only consideration for interaction.

4.2 Further Interactive Models

Building upon this interaction-driven model, further models can be considered that extend past this simple interaction effect between substrates [10]. Below are two extended interactive models, that consider a higher-order term $s_1 s_2$ in the denominator. This captures the idea that substrate concentrations change the growth rate concurrently, supporting the existence of more complex, interdependent relationships between substrates.

$$\mu(s1, s2) = \frac{\mu_{m;1} s_1}{(K_{s;1} + s_1)(1 + \frac{s1}{K_{s;2}})} + \frac{\mu_{m;2} s_2}{(K_{s;2} + s_2)(1 + \frac{s1}{K_{s;1}})} \quad (19)$$

$$\mu(s1, s2) = \frac{\mu_{m;1} s_1}{K_{s;1} + s_1(1 + \frac{s1}{K_{s;2}})} + \frac{\mu_{m;2} s_2}{K_{s;2} + s_2(1 + \frac{s_1}{K_{s;1}})} \quad (20)$$

Both equations consider interaction to a higher degree than that of the generalised interaction model, by incorporating the higher-order interaction term of $s_1 s_2$, however equation 20 neglects the proportion of saturation effects between the two substrates.

5 Quantitative Comparison of Models

Having explored a range of models that aim to capture mixed-substrate bacterial growth, we can now directly compare the suitability of all models using a common measure. As established earlier in equation 3, steady state conditions are reached when the specific bacterial growth rate μ is equivalent to the dilution rate D. Thus, for each model, we can calculate the specific bacterial growth rate at steady state, and compare this with the experimental dilution rate to determine validity.

Table 5 shows the equations used to calculate the specific bacterial growth rate in the experiments for each of the models. Note that the specific bacterial growth rate equation according to the Lendenmann Equation is derived via rearrangement of equation 9 to solve for D, yielding an expression in terms of variables related to the first substrate only. In the analysis we present, the specific growth rate equation for the Lendenmann model is an average of the growth rates obtained for substrate 1 and substrate 2 for each experiment.

Model (Equation)	Growth Relation
Sequential Uptake (6)	$\mu = \frac{\mu_{m;1}\tilde{s}_1}{K_{s;1}+\tilde{s}_1} + \frac{\mu_{m;2}\tilde{s}_2}{K_{s;2}+\tilde{s}_2}$
Lendenmann Ratio (9)	$\mu_1 = \frac{\tilde{s}_1 \sum_{i=1}^{n} s_{0;i}\mu_m}{\tilde{s}_1 \sum_{i=1}^{n} s_{0;i} + s_{0;1} K_s}$
Yoon Interaction (17)	Eq. (17)
Ext. Interaction 1 (19)	Eq. (19)
Ext. Interaction 2 (20)	Eq. (20)

Table 5: The specific growth rate equations for each model presented in this report (the case where $\mu = D$). The relations for the Lendenmann and Sequential Uptake models have been obtained via re-arrangement of the equation for the steady-state substrate concentration, $\tilde{s}$.

Applying the equations in table 5 to the dataset, values for D can be calculated for each model. Then, the sum of square deviations between the experimental dilution rate (the specific growth rate) and the model prediction, $\sum (D_{exp} - \mu_{pred})^2$, can be calculated for each dual-substrate experiment, the results of which can be found below in table 6.

Rows	Eq. 6	Eq. 9	Eq. 17	Eq. 19	Eq. 20
1-6	0.041	0.091	0.006	0.008	**0.001**
19-24	0.092	0.021	0.025	0.099	**0.014**
25-30	0.170	0.064	0.083	0.201	**0.050**

Table 6: Sum of square deviations between the experimental dilution rate and model predictions $\sum (D_{exp} - \mu_{pred})^2$. The bold entries are the lowest values for each row, signifying which model prediction is closest to the experimental data.

In table 6, the values for the sum of square deviations are fairly minimal, suggesting that all models are suitable to an extent in predicting the specific bacterial growth rate in steady-state conditions. Importantly, the bold fields in the table indicate the model which provided the closest match to the experimental values for each experiment. In

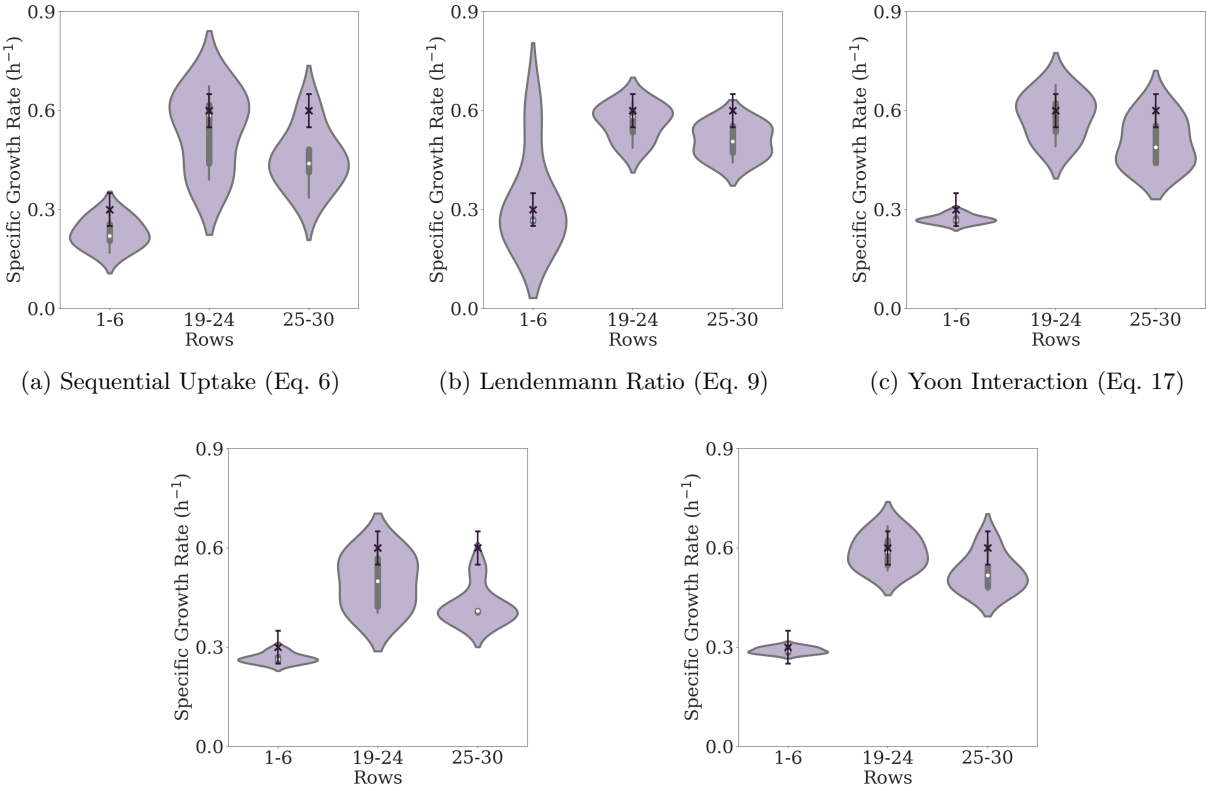

(a) Sequential Uptake (Eq. 6)

(b) Lendenmann Ratio (Eq. 9)

(c) Yoon Interaction (Eq. 17)

(d) Extended Interaction 1 (Eq. 19)

(e) Extended Interaction 2 (Eq. 20)

Figure 3: Violin plots for each of the 5 models explored. The specific growth rate at steady state was calculated for each experiment (Rows 1-6, 19-24, 25-30) using the 5 different growth rate models. The purple violin plots represent the distribution of all the specific bacterial growth rates calculated, and the crosses show the actual experimental dilution rate, with an uncertainty of 5%. In all cases, the experimental dilution rate falls within the bounds of the distribution.

all three cases, this is equation 20.

The extended interaction model 2 (equation 20) is similar to the generalised interaction model proposed by Yoon et al, but incorporates an additional higher-order interactive relationship between the substrates not present in the Yoon model, described by the term $s_1 s_2$ in the denominator. This extended model better captures the underlying mutualistic relationship between the pairs of substrates, as shown by the minimal deviation between experimental values and theoretical predictions for the dilution rate.

In order to visually interpret the suitability of the different models at predicting the steady state specific growth rate, violin plots can be used to show the calculated distributions of the dilution rates for each model. Violin plots provide an insight into the distribution of a set of values, showing the median, quartiles, and overall range of the data. Figure 3 shows a violin plot that has been produced for each of the models, depicting the distribution of theoretically calculated dilution rates for each of the experiments. Additionally, the experimental dilution rates have been indicated using a black cross, with an uncertainty of 5% as stated in Lendenmann's 1994 thesis [7].

The plots indicate that all models are suitable in predicting the specific growth rate in steady-state conditions, with the actual experimental dilution rate (accounting for experimental uncertainty) falling within the distribution bounds of results in all cases. The violin plots reaffirm the greater validity of the interaction models as established through the lower sum of square deviation results, as the distribution bounds are smaller. This suggests that the calculated values for the specific growth rate are very similar to the experimental dilution rate, especially for equation 20.

6 Conclusion

In summary, this report explored a variety of different models that aim to capture the dynamics of mixed-substrate bacterial growth in a chemostat. Starting off with the very rudimentary assumption that bacteria sequentially take up different substrates based on which provided the highest growth rate, we then progressed to a model where the steady state concentration for each individual

substrate was proportional to their input concentrations. Finally, we explored a range of models that accounted for the interaction effect between each individual substrate in the mixture, and these models were generally better in predicting the bacterial growth rate found in the experimental data, especially the model represented by equation 20. These results show that the introduction of higher-order, interaction-accounting growth rate models more accurately reflect the experimental data, suggesting greater suitability in modelling mixed-substrate growth.

Perhaps we can consider these various multi-substrate growth modes as corrective terms to the single substrate growth mode, giving rise to different bounds on the existing steady state. We have already shown that the higher-order models are more suitable in modelling mixed-substrate bacterial growth, and looking beyond this research, there is scope for developing growth models that can account for even higher-order interactions between more substrates.

References

[1] Rosalind J Allen and Bartlomiej Waclaw. Bacterial growth: a statistical physicist's guide. *Reports on Progress in Physics*, 82(1):016601, January 2019.

[2] Manfred Zinn, Thomas Egli, Christoph Herwig, and Atul Narang. Editorial: Recent Advances in Continuous Cultivation. *Frontiers in Bioengineering and Biotechnology*, 9:641249, 2021.

[3] Jacques Monod. Recherches sur la croissance des cultures bacte'riennes (Studies on the growth of bacterial cultures). 911:1–215, 1942.

[4] D. Herbert, R. Elsworth, and R. C. Telling. The Continuous Culture of Bacteria; a Theoretical and Experimental Study. *Journal of General Microbiology*, 14(3):601–622, July 1956.

[5] U. Lendenmann, M. Snozzi, and T. Egli. Kinetics of the simultaneous utilization of sugar mixtures by Escherichia coli in continuous culture. *Applied and Environmental Microbiology*, 62(5):1493–1499, May 1996.

[6] Urs Lendenmann and Thomas Egli. Kinetic models for the growth ofEscherichia coli with mixtures of sugars under carbon-limited conditions. *Biotechnology and Bioengineering*, 59(1):99–107, July 1998.

[7] H. Senn, U. Lendenmann, M. Snozzi, G. Hamer, and T. Egli. The growth of Escherichia coli in glucose-limited chemostat cultures: a re-examination of the kinetics. *Biochimica Et Biophysica Acta*, 1201(3):424–436, December 1994.

[8] Mpho Muloiwa, Stephen Nyende-Byakika, and Megersa Dinka. Comparison of unstructured kinetic bacterial growth models. *South African Journal of Chemical Engineering*, 33:141–150, July 2020.

[9] H. Yoon, G. Klinzing, and H. W. Blanch. Competition for mixed substrates by microbial populations. *Biotechnology and Bioengineering*, 19(8):1193–1210, August 1977.

[10] Gideon Okpokwasili and C.O. Nweke. Microbial growth and substrate utilization kinetics. *African Journal of Biotechnology*, 5:305–317, February 2006.

Appendix

In these experiments, the growth of *E. coli* on mixtures of different substrates was investigated for various substrate ratios at a constant dilution rate, and the steady state concentrations for each substrate were measured. A more concrete description of each experimental dataset can be found below, along with the rows in the dataset that each experiment corresponds:

- **Rows 1-6**: Observing the growth of *E. coli* on a mixture of glucose and galactose for varying substrate ratios at a fixed dilution rate, measuring the steady state concentration of both substrates.
- **Rows 7-12**: Observing the growth of *E. coli* on a mixture of glucose, galactose and fructose, with a fixed dilution rate and fructose concentration, but with varying substrate ratios of glucose to galactose. The steady state concentration of all three substrates was measured.
- **Rows 13-18**: Observing the growth of *E. coli* on a mixture of glucose, galactose, maltose, ribose, arabinose and fructose for varying substrate ratios at a fixed dilution rate, measuring the steady state concentration of all substrates.
- **Rows 19-24**: Observing the growth of *E. coli* on a mixture of glucose and ribose for varying substrate ratios at a fixed dilution rate, measuring the steady state concentration of both substrates.

- **Rows 25-30**: Observing the growth of *E. coli* on a mixture of glucose and fructose for varying substrate ratios at a fixed dilution rate, measuring the steady state concentration of both substrates.

In this report, the DW (Dry Weight) measurement found in the dataset has been interpreted as the bacterial steady state concentration, $\tilde{\rho}$.

Table III. Data used for evaluation of ''mixed substrate models''. Steady-states; 1–6, glucose/galactose mixtures (I); 7–12, glucose/galactose/fructose mixtures (II); 13–18, glucose/galactose/maltose/ribose/arabinose/fructose mixtures (III); 19–24, glucose/ribose mixtures (IV); 25–30, glucose/fructose mixtures (V).

Steady-state	D	DW	$S_{o,\mathrm{Glc}}$	$S_{o,\mathrm{Gal}}$	$S_{o,\mathrm{Mal}}$	$S_{o,\mathrm{Rib}}$	$S_{o,\mathrm{Ara}}$	$S_{o,\mathrm{Fru}}$	s_{Glc}	s_{Gal}	s_{Mal}	s_{Rib}	s_{Ara}	s_{Fru}
1	0.3	4.8	10	0					34	0				
2	0.3	4.5	8	2					25	6				
3	0.3	4.4	6	4					21	13				
4	0.3	4.2	4	6					13	22				
5	0.3	5.3	2	8					7	28				
6	0.3	6.0	0	10					2	39				
7	0.3	6.7	0	10				5	0	29				48
8	0.3	6.4	2	8				5	6	26				47
9	0.3	6.7	4	6				5	10	21				37
10	0.3	6.6	6	4				5	20	10				48
11	0.3	6.7	8	2				5	22	5				38
12	0.3	6.7	10	0				5	25	0				42
13	0.6	47.9	50	10	10	10	10	10	39	8	28	30	43	61
14	0.6	46.4	10	50	10	10	10	10	19	69	28	33	53	73
15	0.6	50.5	10	10	50	10	10	10	12	11	109	31	45	63
16	0.6	47.4	10	10	10	50	10	10	10	12	16	187	49	69
17	0.6	47.9	10	10	10	10	50	10	13	13	32	37	256	81
18	0.6	47.4	10	10	10	10	10	50	9	11	17	31	51	254
19	0.6	49.3	90			10			200			35		
20	0.6	46.5	50			50			37			169		
21	0.6	45.8	50			50			48			178		
22	0.6	44.5	20			80			25			480		
23	0.6	45.7	10			90			16			750		
24	0.6	47.0	5			95			5			820		
25	0.6	47.8	90					10	142					30
26	0.6	47.0	50					50	82					140
27	0.6	47.8	50					50	42					80
28	0.6	44.3	10					90	9					180
29	0.6	46.3	10					90	10					180
30	0.6	48.3	50					50	75					109

Note. D, dilution rate, h^{-1} (accuracy ± 5%). DW, dry weight of cells in the culture, mg L^{-1}. Columns 4 to 9, medium composition in the feed. Columns 10 to 15, steady-state concentrations in the culture. Empty spaces, sugar not present in the mixture. Experiments are described in detail in (Lendenmann et al., 1996). S_o values are in mg L^{-1}, and s values are in μg L^{-1}.

Figure 4: Dataset for the growth of E. coli in a chemostat on various sugar mixtures. Dataset is from Lendenmann and Egli 1998 [6], from the experimental work of Lendenmann, Snozzi and Egli 1996 [4].

Table II. Kinetic parameters of batch and chemostat growth of *E. coli* on the sugars used in this study.

Sugar	μ_{max} (h^{-1})	K_s (μg L^{-1})	Reference
Glucose	0.92	73	Senn et al., 1994
Galactose	0.92	98	Lendenmann, 1994
Maltose	0.87	100	Lendenmann, 1994
Ribose	0.57	132	Lendenmann, 1994
Arabinose	0.73	147	Lendenmann, 1994
Fructose	0.70	125	Lendenmann, 1994

Note. μ_{max}, maximum specific growth rate observed in batch culture. K_s values were obtained by fitting the Monod model to the experimental data using μ_{max} values obtained from batch growth.

Figure 5: Substrate-specific information supplementary to the dataset presented in figure 4, from Lendenmann and Egli 1998 [6]